Plasmonic color pixels fabricated by nanoimprint process

Minoru Takeda[1] · Ryo Takahara[1] · Noriyuki Hasuike[1]

Abstract

Plasmonic nanostructures or metasurfaces have recently been actively researched for structural color generation. Controlling the plasmonic resonant wavelengths of surface plasmon polaritons excited along the metal dielectric interfaces, arising from the resonant interaction with incident electromagnetic waves, reflection or transmission color can be effectively tuned in the visible wavelength region. However, the plasmonic structures are conventionally fabricated by electron beam lithography or focused ion beam, both so expensive and unproductive that they are not practical for large-scale production. In this report, we demonstrate a simple plasmonic nanostructure for various color generation fabricated by a quite simple and cost-effective method applying nanoimprint process and aluminum film deposition. We experimentally evaluated the reflectance spectra of the color pallets composed of the plasmonic nanostructures (plasmonic color pixels) and compared with the simulation results. We confirmed the wide-range tuning ability of reflection color by changing the size parameter of the plasmonic nanostructures. Therefore, this method for high-definitive color generation can be expected to be applied to a wide range of fields including various applications, such as security labels, anti-counterfeiting devices, information storage and functionalized decoration.

Keywords Plasmonic nanostructure · Surface plasmon resonance · Nanoimprint process · FDTD simulation

1 Introduction

Recently, plasmonic nanostructures or metasurfaces have been very actively researched for structural color generation, which was earlier realized by photonic crystals, inspired by natural beauty of form, for example, Morpho didus butterfly wings with a brilliant blue color generated by light interference in their nanostructured scales [1–3].

Printing color using plasmonic (metallic) nanostructures has several advantages over the conventional pigment or dye-based coloration in terms of printing resolution, durability and resource requirements [4–8]. Controlling the absorption peak wavelength of plasmonic resonances, which are standing waves of surface plasmon polaritons excited along the metal dielectric interfaces, arising from the resonant interaction with incident electromagnetic waves, reflection or transmission color can be effectively tuned in the entire visible wavelength region. Confining plasmon modes to small volumes specified by the metallic nanostructures enables subwavelength color printing. High-resolution color-printing technology is very promising for various applications, such as security labels, anti-counterfeiting devices, information storage and functionalized decoration.

However, in conventional research, the plasmonic structures for color generation generally need to be pre-designed and patterned by electron beam lithography (EBL) or focused ion beam (FIB) milling, both so expensive and unproductive that they are not practical for large-scale production. Nanoimprint lithography (NIL) has received much attention recently as one of the next generation nano-lithography methods because of its simple process, low cost and high throughput compared to EBL or FIB [9–11].

In this study, we designed microcolor pallets with various colors generated comprising a simple plasmonic nanostructure fabricated by applying ultraviolet nanoimprint lithography (UV-NIL) [12–14]. We evaluated the reflectance spectra of the color pallets and compared with finite difference

✉ Minoru Takeda
  takeda@kit.ac.jp

1 Department of Electronics, Kyoto Institute of Technology, Matsugasaki, Sakyou-ku, Kyoto 606-8585, Japan

time domain (FDTD) simulation results. The plasmonic nanostructure is quite simple and easy to fabricate using the high-throughput nanoimprint process with very low cost compared to the conventional fabrication method, such as an EBL.

2 Experimental methods

Schematics of the plasmonic nanostructure we designed are shown in Fig. 1. The unit pixel (element) is composed of the square blocks (pillar shape) made of UV curable resin on silicon (Si) substrates which are covered by thin aluminum (Al) film. The size of the square blocks and pixels which are arranged periodically determines the spectral characteristics. Various color-generating pallets which consist of ten thousand pixels (100×100) are obtained by changing block size L and pixel size P which determine visible spectra specified by plasmonic resonance. The sizes of the pixel P and block size L are changed from 400 nm to 560 nm and 260 nm to 420 nm with an increment of 40 nm, respectively. So, the gap sizes between the square blocks are maintained at 140 nm.

In the fabrication process of the plasmonic nanostructure, we applied UV-NIL as illustrated in Fig. 2. We prepared a transparent silica mold in which the various P and L size concave patterns (inverted shape of the block patterns as shown in Fig. 1) were processed, and used the mold to transfer the patterns to the UV curable resin using UV-NIL on Si substrate. First, the UV resin is spin-coated and baked
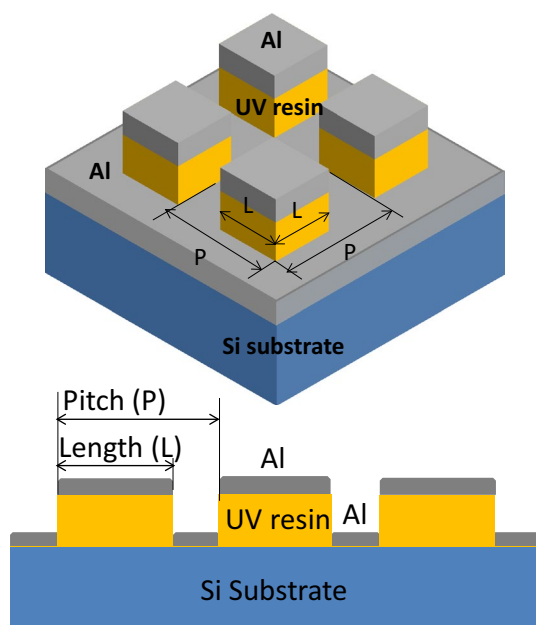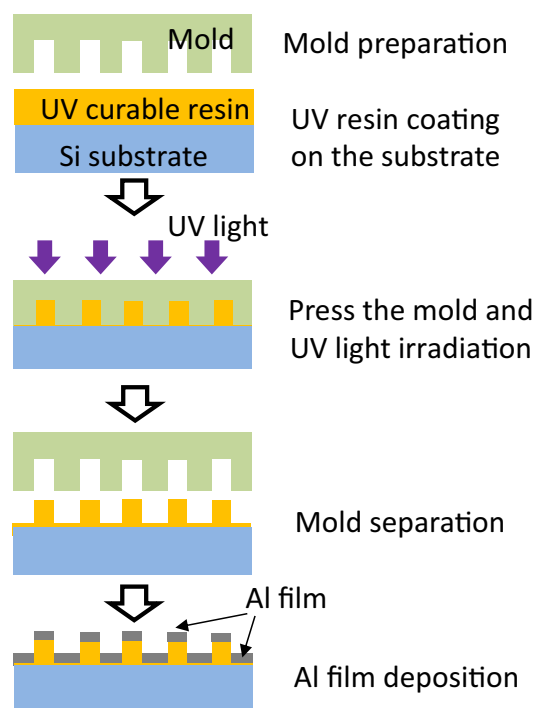

Fig. 2 (Color online) Schematic diagram of the fabrication process

on substrate so that its film thickness is around 200 nm. Then, the silica mold is pressed on to the UV resin under 1.0 MPa constant pressure and UV light is irradiated with power density 70 mW/cm^2 for 60 s. Figure 3 shows scanning electron microscopy (SEM) images of the two-dimensional (2D) array of the pillar (convex)-shaped UV resin patterns in the actually fabricated samples with various sizes of P and L as indicated in each image. Fine patterns are successfully fabricated on the substrate. The pillar height is about 150 nm, which is estimated by the AFM measurements of the sample. Finally, Al film of 40 nm thickness is formed on the 2D array structures as illustrated in Fig. 1 by sputtering method using Sanyu Electron SC-701Mk2.

3 Results and discussion

We simulated the reflectance spectra and the electric field distribution of the plasmonic nanostructure of various P and L values as shown in Fig. 1 using a FDTD solver (Science and Technology Institute KeyFDTD) to estimate the spectral behavior and analyze the plasmonic resonance.

In the simulation, periodic boundary conditions were implemented in the x and y directions, which are normal to the sample surface and perfectly matched layer (PML) boundary conditions were implemented in the x–y plane on the top and bottom of the sample surface. The reflectance was calculated using normally incident (z direction) plane

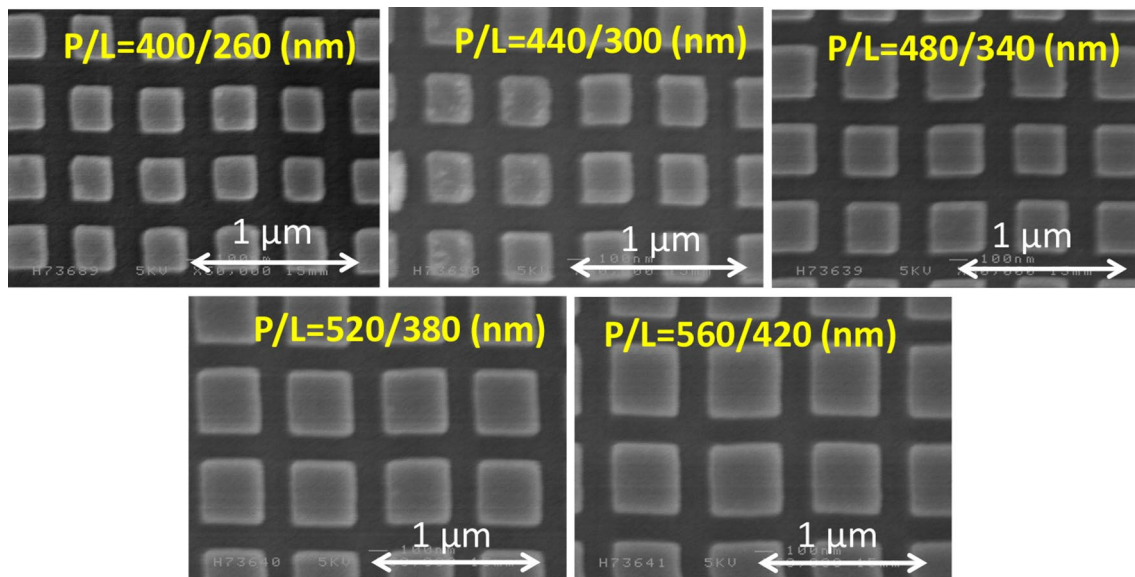**Fig. 1** (Color online) Schematic of a plasmonic nanostructure

Fig. 3 SEM images of square block patterns fabricated by nanoimprint lithography using UV curable resin
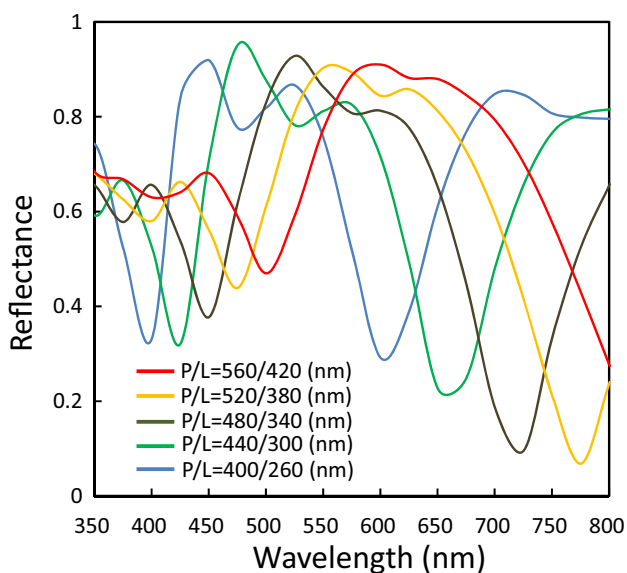

Fig. 4 (Color online) Simulation results of reflectance spectra of the 2D pixel arrays with various P/L size

wave which is linear polarized onto the sample surface. Since the Si substrate transmits almost no light, the plasmonic structure absorbs all but reflected light.

Figure 4 shows the simulated reflectance spectra of the 2D pixel arrays composed of five sets of P/L values. Two resonance wavelengths of reflectance dips can be seen in each structure. The shorter resonance wavelength corresponds to the pixel size P, which is the periodicity. The longer one is thought to be originated from the localized surface plasmon resonance (LSPR) supported by the Al square patch on the block and the wavelength is determined by the block size L. Increasing the P and L with the same gap size between the blocks results in the red shift of the two dip wavelengths and the peak one between them, enabling a wide-range tuning of reflection color in the visible region.

Figure 5 shows simulation results of resonance dip shifts of the 2D pixel arrays. In Fig. 5a, D1 is the wavelength of the shorter resonance dip and D2 is the wavelength of longer one, with varying the block size L from 220 nm to 300 nm and fixing the pixel size P to 400 nm. D1 keeps almost the same value, whereas D2 changes in the range of about 80 nm. Therefore, the longer resonance dip (D2) is attributed to the LSPR determined by the block size L. In Fig. 5b, shifts of D1 and D2 are similarly plotted with varying the pixel size P from 360 nm to 440 nm and fixing the block size L to 260 nm. D1 changes in the range of about 80 nm corresponding to the change of the pixel size. On the other hand, D2 changes by about 30 nm. This small change may be affected by the shift of D1, but further studies are needed.

The simulated electric field distributions in the pixel of P/L = 400/260 nm at 450 nm and 600 nm wavelengths, corresponding to the peak and dip reflectance are illustrated in Fig. 6. The strong LSPR supported by the Al patch is demonstrated for 600 nm wavelength (reflectance dip). The enhanced electric field can be seen between the upper Al patch and the bottom Al layer that is inside the UV resin. The highly confined electric field is considered to be caused by the strong LSPR combined with the bottom Al layer, which brings about increased light absorption [15]. On the other hand, the upper Al patch works as a radiating dipole antenna and relatively weak electric fields are seen inside the UV resin at 450 nm wavelength (reflectance peak).

Fig. 5 (Color online) Simulation results of resonance dip shifts of the 2D pixel arrays **a** with varying L and fixed P, and **b** with varying P and fixed L, D1 is the shorter resonance dip and D2 is the longer resonance one
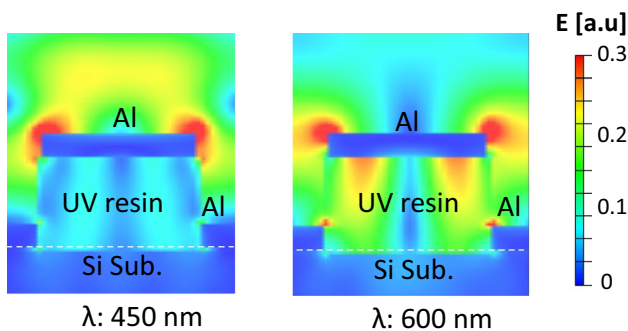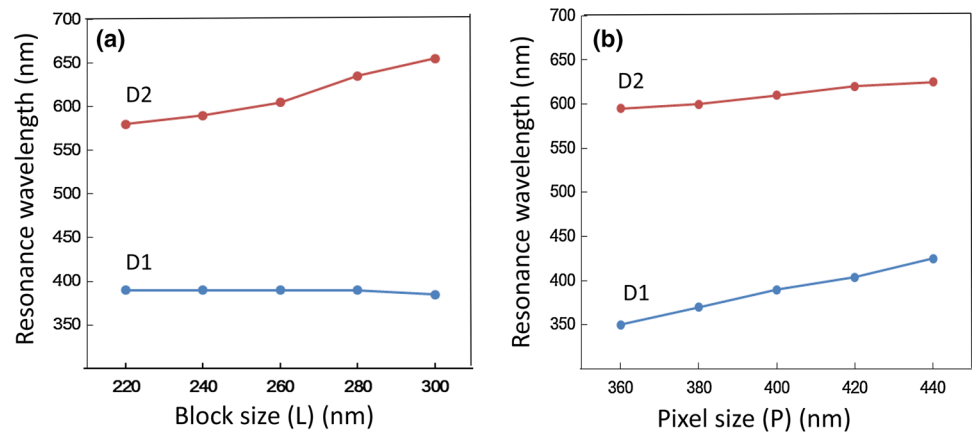

Fig. 6 (Color online) Electric field distributions in the pixel structures of P/L = 400/260 nm at 450 nm and 600 nm wavelengths irradiation
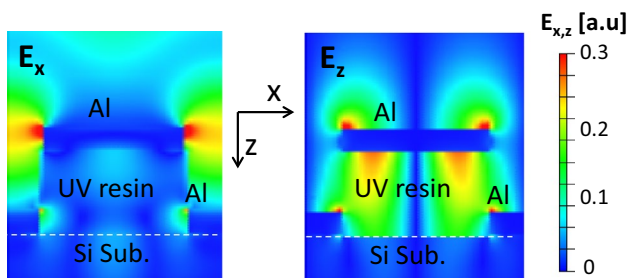

Fig. 7 (Color online) Electric field distributions of E_x and E_z components in the pixel structures of P/L = 400/260 nm at 600 nm wavelength irradiation

Fig. 8 (Color online) Experimental reflectance spectra of the color pallets with variou

The electric field distributions of E_x and E_z components are plotted in Fig. 7 for further understanding the resonance phenomena at 600 nm wavelength. The direction of E_x is the same as the electric field of the incident light. The enhanced regions of E_x represent the dipole resonance of the LSPR excited in the upper Al patch. Regarding E_z distribution, the strongly enhanced regions can be seen inside the UV resin and edges of the bottom Al layer, with the enhanced region on the Al patch surface. So, the highly confined electric field
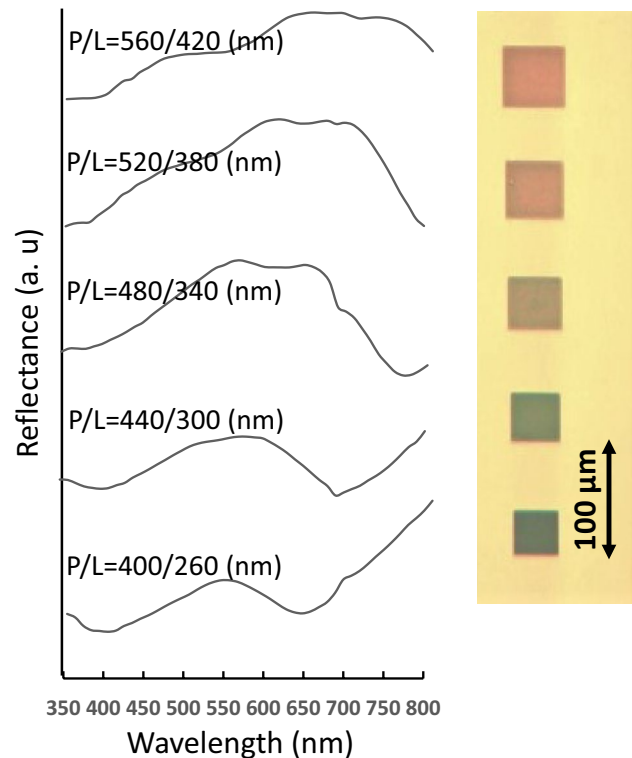
inside the UV resin is brought by the strong interaction of E_z component between the upper Al patch and the bottom Al layer.

Reflectance spectra of the actually fabricated color pallets composed of the 2D pixel arrays corresponding to the simulation results are measured using a microscopic spectrophotometer (JASCO MSV-5200). Figure 8 shows the measured reflectance spectra of the color pallets of each P/L value pixels. Spectral reflectance of each condition is offset on the vertical axis to make it easier to see clearly. Optical microscope images of corresponding color pallets are also

lined up on the right hand, generating blue, green and red colors. The measured spectral features generally agree to the simulation results. So, we experimentally confirmed the wide-range tuning ability of reflection color by changing the size parameter of the plasmonic nanostructures composing the microcolor pallets. Two dip wavelengths and the peak one between them predicted by the simulation described above are clearly observed for the two smaller P/L value pixels and the wavelength of the peak reflectance shifts to longer wavelength as P/L values increase. As for the larger P/L value pixels, two dip wavelengths are not so clear mainly due to the structural size deviation from the designed values and the fabrication imperfection.

4 Conclusion

We designed microcolor pallets composed of plasmonic nanostructures and fabricated them by applying nanoimprint process. We experimentally confirmed the wide-range tuning ability of reflection color by changing the size parameter of the plasmonic nanostructures. The structure is quite simple and can be manufactured at very low cost by applying nanoimprint process and using aluminum as a cheap and abundant metal. It is also possible to form plasmonic nanostructure patters on a flexible substrate, such as a plastic film, by modifying the fabrication process shown in this study. Therefore, this method can be expected to be applied to a wide range of fields including high-definition color printing.

References

1. Watanabe, K., Hoshino, T., Kanda, K., Haruyama, Y., Kaito, T., Matsui, S.: Optical measurement and fabrication from a Morpho-butterfly-scale quasistructure by focused ion beam chemical vapor deposition. J. Vac. Sci. Technol. B **23**(2), 570 (2005)
2. Kinoshita, S., Yoshioka, S., Miyazaki, J.: Physics of structural colours. Rep. Prog. Phys. **71**, 076401 (2008)
3. Sun, J., Bhushan, B., Tong, J.: Structural coloration in nature. RSC Adv. **3**, 14862 (2013)
4. Xu, T., Wu, Y., Luo, X., Guo, L.: Plasmonic nanoresonators for high-resolution colour filtering and spectral imaging. Nat. Commun. **1**, 59 (2010)
5. Kumar, K., Duan, H., Hegde, R.S., Koh, S.C.W., Wei, J.N., Yang, J.K.W.: Printing colour at the optical diffraction limit. Nat. Nanotechnol. **7**, 557 (2012)
6. Tan, S.J., Zhang, L., Zhu, D., Goh, X.M., Wang, Y.M., Kumar, K., Qiu, C., Yang, J.K.W.: Plasmonic color palettes for photorealistic printing with aluminum nanostructures. Nano Lett. **14**, 4499 (2014)
7. Zhu, X., Vannahme, C., Nielsen, E., Mortensen, N., Kristensen, A.: Plasmonic colour laser printing. Nat. Nanotechnol. **11**, 325 (2016)
8. Mudachathi, R., Tanaka, T.: Up scalable full color plasmonic pixels with controllable hue, brightness and saturation. Sci. Rep. **7**, 1199 (2017)
9. Miyata, M., Hatada, H., Takahara, J.: Full-color subwavelength printing with gap-plasmonic optical antennas. Nano Lett. **16**, 3166 (2016)
10. Duan, X., Kamin, S., Liu, N.: Dynamic plasmonic colour display. Nat. Commun. **8**, 14606 (2017)
11. Nagasaki, Y., Hotta, I., Suzuki, M., Takahara, J.: Metal-masked MIE-resonant full-color printing for achieving free-space resolution limit. ACS Photonics **5**(9), 3849 (2018)
12. Chou, S.Y., Krauss, P.R., Renstrom, P.J.: Imprint of sub—25 nm vias and trenches in polymers. Appl. Phys. Lett. **67**, 3114 (1995)
13. Vratzov, B., Fuchs, A., Lemme, M., Henschel, W., Kurz, H.: Large scale ultraviolet-based nanoimprint lithography. J. Vac. Sci. Technol. B **21**(2), 2760 (2003)
14. Mano, I., Taniguchi, J.: Fabrication of an antireflection structure on an aspherical lens using a UV-curable inorganic–organic hybrid polymer. Jpn. J. Appl. Phys. **58**, SDDJ03 (2019)
15. Li, W., Hu, J., Chou, S.: Extraordinary light transmission through opaque thin metal film with subwavelength holes blocked by metal disks. Opt. Express **19**, 21098 (2011)